北見工業大学研究報告
第14巻 第1号 (昭和57年)

Memoirs of the Kitami Institute of Technology
Vol. 14 No. 1 (1982)

A Behavior of Ice Growth around a Horizontal Cylinder in Water Flow

by Hideo INABA*

(Received April 15, 1982)

Abstract

The behavior of ice growth around a horizontal cylinder in cold water flow is studied experimentally for the ranges of Reynolds numbers $Re_d=2.3\times10^2\sim8.6\times10^4$ and cooling temperature ratios $\theta_c=6.3\sim75.8$. The local and average heat transfer coefficients at the ice-water interface are obtained from measured ice profiles by using a series solution of the Laplace equation in the ice layer. Correlation equations for the average heat transfer are obtained for three regimes of Reynolds numbers. A correlation is also obtained for the cooling capacity that can be stored in the ice layer around a cylinder.

Nomenclature

A_s : cross- sectional area of ice
a_n, b_o : coefficients of series solution in eq. (3)
c_p : specific heat
Ds : effective diameter of ice near forward stagnation point
$D_{\max}$: maximum diameter of ice layer profile
d : cylinder diameter
Gr_{Ds} : Grashof number
H : height of rectangular test section
h_m, $h_{n,\phi}$: average and local heat transfer coefficients
k_i, k_w : thermal conductivities for ice and water
L : latent heat of fusion per unit volume
Nu_d, Nu_{Ds} : average Nusselt number $=h_m d/k_w$, $h_m Ds/k_w$
Pr : Prandtl number
Q : cooling capacity stored in ice layer per unit axial length
Q' : nondimensional cooling capacity
R, R_1, R_2 : radial coordinate, outside radius of cylinder and radial coordinate of ice-water interface
Re_d, Re_{Ds} : Reynolds number $=U_\infty d/\nu$, $U_\infty Ds/\nu$
r : dimensionless radial coordinate $=R/R_1$
T : temperature
T_f, T_w, T_∞ : freezing temperature of water, surface temperature of cylinder and free stream temperature

* Department of Mechanical Engineering, Kitami Institute of Technology

Tu : longitudinal (streamwise) turbulence intensity $=(U'^2)^{1/2}/U_\infty$
U_∞ : free strem velocity
$(U'^2)^{1/2}$: r. m. s. — value of longitudinal fluctuating velocity component
γ_s : density of ice
θ : dimensionless temperature $=(T-T_w)/(T_f-T_w)$
θ_c : cooling temperature ratio $=(T_f-T_w)/(T_\infty-T_f)$
ν : kinematic viscosity
ϕ : angular position measured from forward stagnation point
ψ : angle defined in Fig. 2.

1. Introduction

The classical Stefan problems or free boundary problems in which diffusive processes control the change of phase of a material occur in many scientific and engineering problems involving natural phenomena and industrial processes. Recent extensions of the Stefan problem motivated largely by practical applications consider such real effects as convection (free and/or forced), flow regime (laminar or turbulent), maximum density, supercooling, geometrical configurations, multi-dimensionality and other physical effects involving either extrenal or internal flow situations. Since the literature on the Stefan problem and its generalized variations or extensions including both theoretical and experimental studies is voluminous, it suffices here to mention the related monographs[1~6] and some review articles[7~12]. Because of the difficulty in obtaining analytical solutions for the free boundary problems, it is expected that the development of numerical solutions using either finite difference or finiteel ement technique will be of continued interest in the future.

For many of the more difficult free boundary problems not even numerical techniques are entirely adequate and one must resort to experimental investigations. This appears to be particularily ture of problems where flow separation, transition to turbulence or a turbulent flow may exist. In such situations[13~16] new phenomena such unstable behavior, not anticipated by theoretical calculations have been observed. Extensive experimental investigations of ice formation in the presence of forced convection flows in pipes[15~18] and along flat plates[19~20] have been reported. Natural convection heat transfer to vertical[21~22] and horizontal[23] ice cylinders has also been investigated. As well the opposite case of melting of a phase change medium by a hot cylinder has recently been studies in connection with thermal storage of solar energy[24,25]. In contrast, only a very limited number of experimental results have been reported for the case of freezing around a cooled pipe in cross flow[26,27] and these results exist only at rather low Reynolds numbers — less than 10^3. Theoretical predictions of ice growth around a cylinder exist only for the case of conduction heat transfer[28,31]. On the other hand, forced convection around a horizontal circular cyliner without phase change is one of the basic problems in convective heat transfer and has been studied extensively by many investigators[32]. Only a few typical experimental

investigations[33~35] will be mentioned here for reference.

When an isothermal cooled long horizontal circular pipe with a wall temperature below the freezing temperature ($T_w < 0°C$) is immersed in flowing water at a uniform temperature $T_\infty > 0°C$, the two-dimensional transient solidification problem arises. In this initial process, the latent heat of fusion is released at the ice-water interface and the ice thickness increases until a steady state is reached. For the range of experimental conditions in this study, the steady state condition is approached within the order of hours after the initiation of the cooling process. In the transient process, the latent heat, the convective heat at the interface and the heat removal to subcool the ice are conducted through the solid into the cooling pipe wall. A steady state is reached when the convective heat transfer is balanced by the conduction heat transfer at the interface. It is the shape of this steady state interface and the convective heat transfer rate there that will be studied here.

2. Experimental Apparatus and Procedure

Experiments were conducted in a closed loop water tunnel having a test section in the form of a rectangular plexiglass channel, measuring 25.4 cm wide, 45.7 cm high and 313.4 cm long. A smooth converging entrance section provides a uniform flow to the section and the velocity can be varied in the range $U_\infty =$ 1 cm/s to 5 m/s. The temperature of the water can be controlled at any value between room temperature and near 0°C by means of a refrigeration and heat

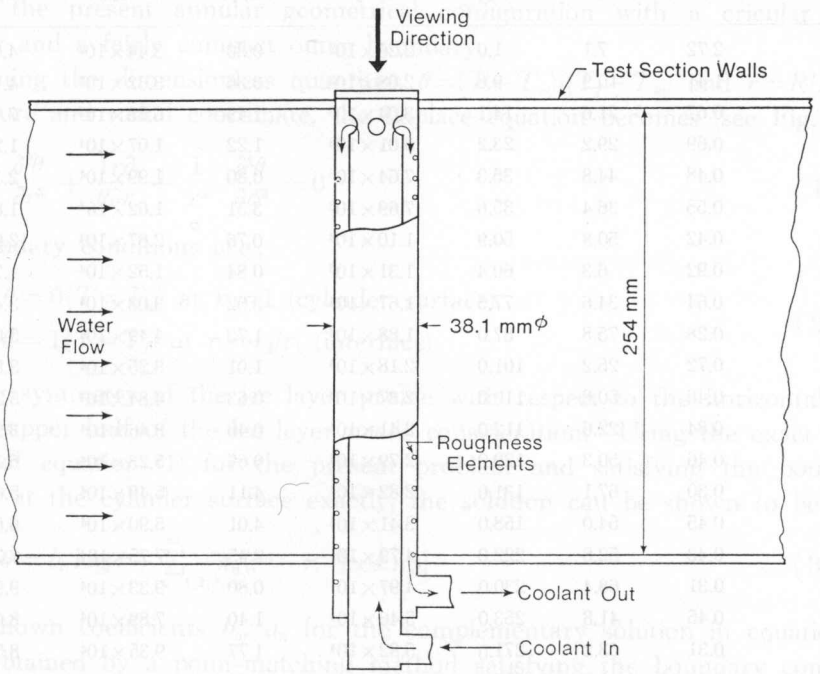

Fig. 1. Test cylinder.

exchanger system. A copper test cylinder (outside diameter 38.1 mm, wall thickness 1.5 mm and length 254 mm) was placed horizontally in the test section. A schematic of the test cylinder details is shown in Fig. 1. To promote turbulence of the coolant (a mixture of glycol, alcohol and water) in the test cylinder for high heat transfer, a coiled spring was inserted in the annnular space. The coolant was circulated at a high velocity between the test cylinder and a temperature controlled bath with a temperature range of $0\sim-25$°C. The inlet and outlet temperatures of the coolant at the test cylinder were within 0.1°C. The two-dimensionality of the flow and temperature fields around the hroizontal cylinder was axially uniform except for a small region near the wall of the rectangular test section.

A calming section with screens is located at a distance 3 m upstream from the test cylinder. Three sizes of screens, $M=22$ mm, $d_g=1.5$ mm, $M=3.5$ mm, $d_g=0.7$ mm, and $M=0.6$ mm, $d_g=0.15$ mm, where $M=$mesh size and $d_g=$ wire diameter, were employed in the present experiments. The free stream velocity and turbulence level were measured at a location about 10 cylinder dimeters upsteram of the test cylinder using a laser Doppler anemometer system (15 mW). The turbulent intensity $Tu=(U'^2)^{1/2}/U_\infty$ was estimated from the streamwise component of the free stream velocity fluctuation. The free stream temperature was also measured at the same location.

Table 1. Range of Parameter Values for Experiments

Sympols	T_∞, °C	θ_c	U_m,	Re_d	Tu, %	Re_{Ds}	$Re_{D\max}$
○	2.72	7.1	1.0	2.26×10^2	0.30	3.44×10^2	4.07×10^2
●	1.41	10.9	9.6	2.08×10^3	0.36	3.62×10^3	4.18×10^3
◑	0.67	21.6	14.1	3.04×10^3	1.49	6.53×10^3	7.46×10^3
◐	0.69	29.2	23.2	5.01×10^3	1.22	1.07×10^4	1.24×10^4
◓	0.48	44.8	35.3	7.64×10^3	0.80	1.99×10^4	2.14×10^4
◒	0.55	36.4	35.6	7.69×10^3	3.51	1.62×10^4	1.89×10^4
□	0.42	50.8	50.9	1.10×10^4	0.76	2.67×10^4	2.98×10^4
■	0.92	6.3	60.4	1.31×10^3	0.84	1.52×10^4	1.79×10^4
◨	0.64	34.6	77.5	1.67×10^4	3.02	3.03×10^4	3.44×10^4
◧	0.28	75.8	87.0	1.88×10^4	1.72	4.49×10^4	5.02×10^4
⬒	0.72	25.2	101.0	2.18×10^4	1.01	3.25×10^4	3.87×10^4
⬓	0.46	50.6	110.0	2.37×10^4	0.63	4.84×10^4	5.21×10^4
◩	0.84	22.6	112.0	2.41×10^4	0.40	3.46×10^4	3.91×10^4
◪	0.46	50.3	129.0	2.79×10^4	0.67	5.23×10^4	6.12×10^4
◹	0.30	67.1	131.0	2.82×10^4	4.11	5.49×10^4	5.61×10^4
◸	0.45	54.0	158.0	3.41×10^4	4.01	5.90×10^4	6.61×10^4
△	0.43	52.8	222.0	4.79×10^4	2.45	7.75×10^4	7.78×10^4
▲	0.31	68.4	230.0	4.97×10^4	0.80	9.33×10^4	9.94×10^4
▽	0.45	41.8	253.0	5.46×10^4	1.40	7.89×10^4	8.07×10^4
▼	0.31	63.2	271.0	5.82×10^4	1.77	9.35×10^4	8.57×10^4
◇	0.44	43.8	397.0	8.57×10^4	1.72	1.17×10^5	1.09×10^5

After reaching a steady state for the given experimental conditions (coolant temperature or the cylinder surface temperature, free stream velocity and temperature), the ice contour was recorded photographically. The data reduction for the local heat transfer coefficient at the ice-water interface and other heat transfer results is based on the photographic record of the ice profile. In this study, the range of the experimental conditions were (see Table 1):

free stream velocity $U_\infty = 1.02 \sim 397$ cm/s
free stream turbulence intensity $Tu = 0.3 \sim 4.0\%$
free stream longitudinal turbulence length scale ratio $l/Ds = 0.48 \sim 5.5$
free stream water temperature $T_\infty = 0.25 \sim 2.7$°C
cylinder surface temperature $T_w = -5.8 \sim -24.2$°C
Reynolds number based on outside diameter of cylinder $Re_d = 2 \times 10^2 \sim 9 \times 10^4$
cooling temperature ratio $\theta_c = 6.3 \sim 75.8$

3. Analysis of temperature field in the ice layer and the determination of the local heat transfer coefficient at the ice-water interface

By noting that the cylinder surface temperature T_w and the freezing temperature $T_f = 0$°C are known, the two-dimensional temperature field of the steady state ice layer can be obtained by a point-matching technique using the exact solution of the Laplace equation in polar coordinates. Past experience suggests that the point-matching method will yield sufficiently accurate approximate solution for the present annular geometrical configuration with a cricular inner boundary and a fairly compact outer boundary.

Defining the dimensionless quantities $\theta = (T - T_w)/(T_f - T_w)$ and $r = R/R_1$ for temperature and radial coordinate, the Laplace equation becomes (see Fig. 2)

$$\frac{\partial^2\theta}{\partial r^2} + \frac{1}{\theta}\frac{r\partial}{\partial r} + \frac{1}{r^2}\frac{\partial^2\theta}{\partial\phi^2} = 0 \qquad (1)$$

The boundary conditions are:

$$\theta = 0 (T = T_w) \text{ at } r = 1 \text{ (cylinder surface)}$$
$$\theta = 1 (T = T_f) \text{ at } r = r_2/r_1 \text{ (interface)} \qquad (2)$$

Assuming symmetry of the ice layer profile with respect to the horizontal axis, only the upper half of the ice layer needs consideration. Using the exact series solution of equation (1) for the present problem and satisfying the boundary condition at the cylinder surface exactly, the solution can be shown to be

$$\theta = b_o \log r + \sum_{n=1,2,3,\cdots}^{\infty} a_n (r^n - r^{-n}) \cos n\phi] \qquad (3)$$

The unknown coefficients b_o, a_n for the complementary solution in equation (3) can be obtained by a point-matching method satisfying the boundary condition $\theta = 1$ at the ice-water interface at twenty equally angular spaced points along the

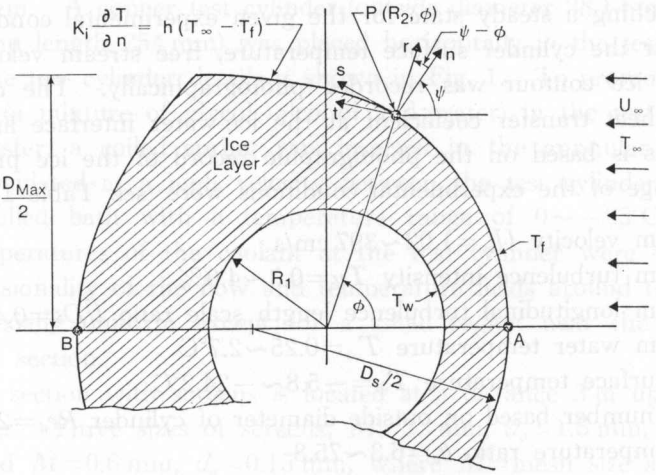

Fig. 2. Definition of variables and coordinates used.

upper ice profile AB (see Fig. 2). For the solution of Laplace equations, it is known that the maximum error occurs at the boundary. Calculations were made for $n=20$, 30 and 40. In view of the rather small difference in results among the thre ecases, $n=20$ was selected in this study. With $n=20$ the maximum boundary errors for θ at the interface were found to be less than 10^{-6} for some extreme cases. In most cases the maximum boundary errors were negligibly small, being of the order of 10^{-9} or less whereas the exact boundary value is $\theta=1$. This observation confirms the convergence of the solution.

With the temperature field for the annular ice layer available, the local and average heat transfer coefficients at both the ice-water interface and the cylinder surface can be computed readily. At steady state, heat balance at the interface gives

$$h(T_\infty - T_f) - k_i \left.\frac{\partial T}{\partial n}\right|_{R=R_2} = 0 \qquad (4)$$

In terms of the dimensionless quantities θ and r defined earlier, the local heat transfer coefficient $h_{n,\phi}$ can be written as

$$h_{n,\phi} = k_i \frac{(T_f - T_w)}{(T_\infty - T_f)} \frac{1}{R_1} \left[\frac{\sin(\psi-\phi)}{r_2} \left.\frac{\partial\theta}{\partial\phi}\right|_{r=r_2} + \cos(\psi-\phi) \left.\frac{\partial\theta}{\partial r}\right|_{r=r_2} \right] \qquad (5)$$

where the angle ψ is defined in Fig. 2. The direction of the external normal n at any point on the ice-water interface was determined by considering the chord subtended by the two neighboring points located at $\pm 2.5°$ from an angle ϕ. By using equation (3) the heat transfer rate through the cylinder surface ($R=R_1$) can be found by integration. On the other hand, the heat transfer rate through the ice-water interface can be obtained by using Simpson's rule for integration. The agreement between the two results was found to be within 1 percent in all cases confirming the accuracy of the present method of determining the local heat transfer coefficient. Precision in measuring the ice layer thickness is

an important factor in the present method for determining the temperature field of the ice layer. In order to minimize the measuring errors the photographs of the ice layer were enlarged two to three times the actual size.

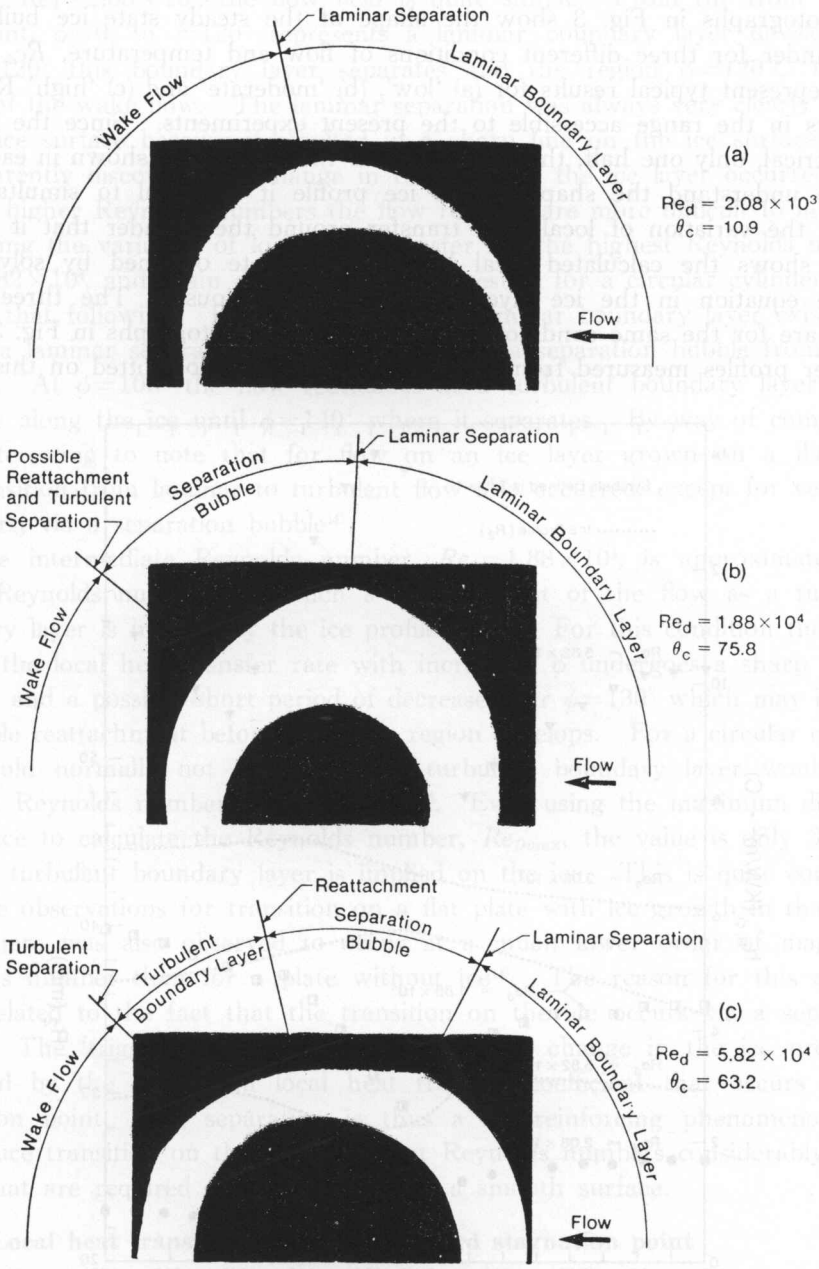

Fig. 3. Photographs of ice layer (light coloured region) around the cylinder at various Reynolds numbers. Flow regions indicated were obtained by an interpretation of the local heat transfer coefficient variation around the cylinder.

4. Experimental results and discussion

4.1 Steady state ice layer profile and local heat transfer at the ice-water interface

Photographs in Fig. 3 show the shape of the steady state ice buildup on the cylinder for three different conditions of flow and temperature, Re_d and θ_c. They represent typical results for (a) 'low', (b) 'moderate' and (c) 'high' Reynolds numbers in the range accessible to the present experiments. Since the ice was symmetrical, only one half, the upper half, of the ice layer is shown in each case.

To understand the shape of the ice profile it is useful to simultaneously look at the variation of local heat transfer around the cylinder that it implies. Fig. 4 shows the calculated local heat transfer rate obtained by solving the Laplace equation in the ice layer as described previously. The three results shown are for the same conditions as existed in the photographs in Fig. 3. The ice layer profiles measured from the photographs are also plotted on this figure.

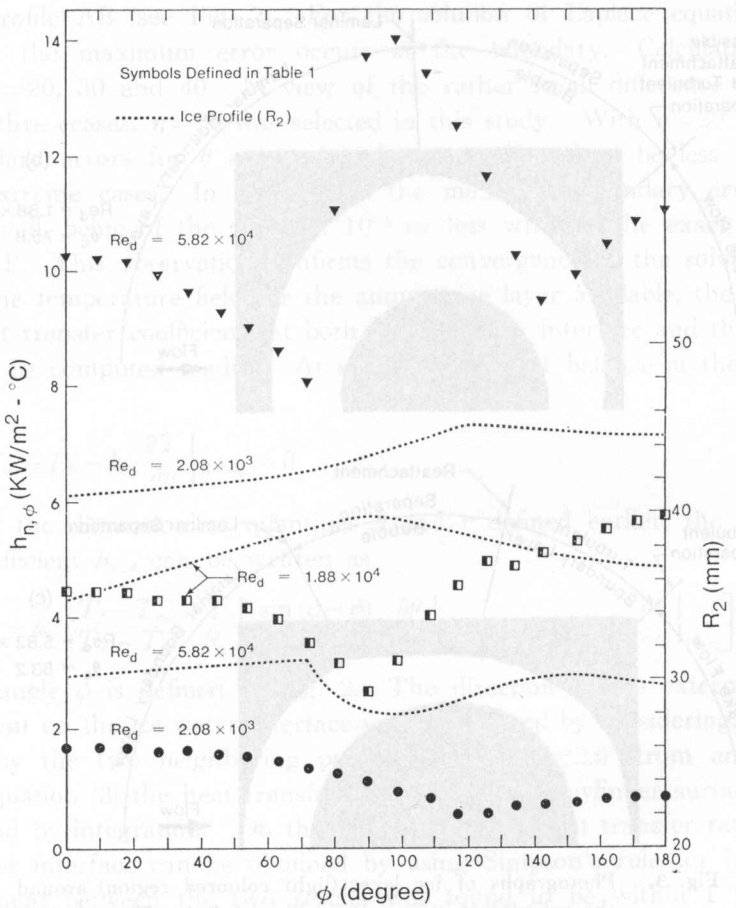

Fig. 4. Variation around the cylinder of the thickness of the ice layer and the local heat transfer coefficient that was calculaed from it.

By examining the ice layer profiles and by comparing the variation in local heat transfer with that observed on a circular cylinder, some speculations can be made about the implied flow regimes around the ice. At the lowest Reynolds number, $Re_d=2.08\times10^3$, the flow field is quite simple. From the front stagnation point, $\phi=0$, to $=120°$ represents a laminar boundary layer development. At $\phi=120°$ this boundary layer separates and the region $\phi=120°$C to $180°$ represent the wake flow. The laminar separation was always very clearly evident in the ice surface because it resulted in a sharp line on the ice surface where an apparently discontinuous change in the slope of the ice layer occurred.

At higher Reynolds numbers the flow regimes are more difficult to interpret. Examining the variation of local heat transfer for the highest Reynolds number, $Re_d=5.82\times10^4$, and again comparing it with results for a circular cylinder would suggest that following. From $\phi=0$ to $70°$ a laminar boundary layer exists. At $\phi=70°$ a laminar separation occurs followed by a separation bubble from $\phi=70$ to $100°$. At $\phi=100°$ the flow reattaches as a turbulent boundary layer which develops along the ice until $\phi=140°$ where it separates. By way of comparison it is interesting to note that for flow on an ice layer grown on a flat plate the transition from laminar to turbulent flow also occurred, except for very thin ice layers, via a separation bubble[14].

The intermediate Reynolds number, $Re_d=1.88\times10^4$, is approximately the lowest Reynolds number for which a reattachment of the flow as a turbulent boundary layer is implied by the ice profile shape. For this condition the variation of the local heat transfer rate with increasing ϕ undergoes a sharp change in slope and a possible short period of decrease near $\phi=130°$ which may indicate a possible reattachment before the wake region develops. For a circular cylinder one would normally not expect that a turbulent boundary layer would exist below a Reynolds number of about 4×10^5. Even using the maximum diameter of the ice to calculate the Reynolds number, $Re_{D\max}$, the value is only 3.9×10^4 when a turbulent boundary layer is implied on the ice. This is quite consistent with the observations for transition on a flat plate with ice growth in that transition there was also observed to occur at a much lower order of magnitude Reynolds number than for a plate without ice[14]. The reason for this appears to be related to the fact that the transition on the ice occurs via a separation bubble. The 'trigger' for the separation, a sharp change in the ice profile, is produced by the change in local heat transfer coefficient that occurs at the separation point. The separation is thus a self-reinforcing phenomenon that can induce transition on the ice surface at Reynolds numbers considerably lower than what are required for a transition on a smooth surface.

4.2 Local heat transfer around the forward stagnation point

From the photographic results of the ice layer profile around the isothermally cooled cylinder, it is found that the ice-water interface can be approximated by a circle near the forward stagnation point with a maximum deviation of $\pm1.5\%$ within the angular position $\phi<45°$. In this region heat transfer rates may be

compared to those for a circular cylinder. Forced convection from a cricular cylinder with constant wall temperature has been studied by Squire[38], Schmidt Wenner[30] and many others. Schmidt and Wenner provide the following experimental correlation equation for the local heat transfer coefficient near the forward stagnation point

$$\frac{h_x d}{k} = 1.14\left(\frac{U_\infty d}{\nu}\right)^{1/2} Pr^{0.4}\left[1-\left(\frac{\varphi^\circ}{90}\right)^3\right] \qquad (6)$$

The average Nusselt numbers $(Nu)_{Ds}=h_m Ds/k_w$, Ds=diameter of a circle near the forward stagnation point, from the present experiments are shown in Fig. 5 and the results are compared with theory[38] and experiment[39]. Although some scatter of the experimental data exists depending on the experimental conditions, the present results are in very good agreement with those in the reference[38,39].

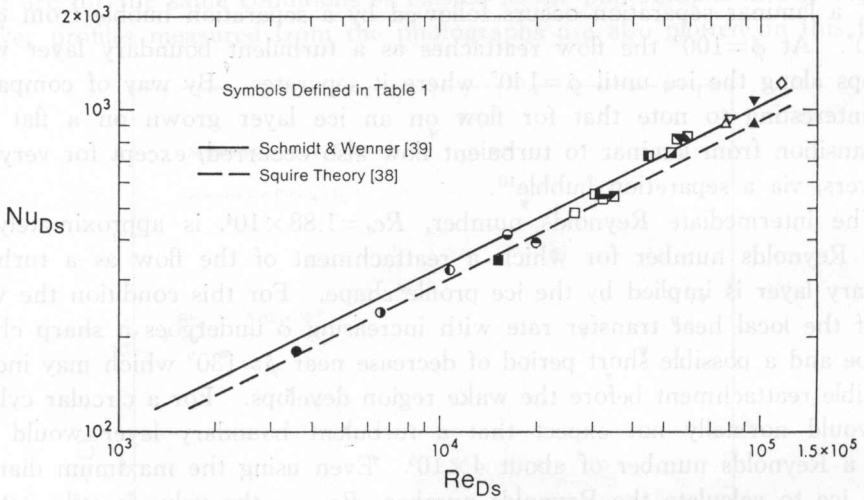

Fig. 5. Comparison of the heat transfer rate at the forward stagnation point on the ice with results for a circular cylinder.

At this point it is of interest to consider the various factors which might contribute to scatter in the present results and to difference in results among various investigations.

A. Variable property effects

Since the temperature difference between the ice surface (0°C) and the free stream is less than 2.7°C in the present investigation, one would not except the effect of variable viscosity to be significant[40]. The main problem comes in comparing the present results with other results obtained using air as a working medium. Scaling the data using $Pr^{0.4}$ as opposed to $Pr^{1/3}$ correlation resluts in a 20 percent difference in the predictions with the former giving the best agreement.

B. Channel blockage effect

The blockage ratio D_{max}/H where D_{max} is the maximum diameter of the ice

and H is the height of the test section reached a maximum value of 0.23. When the results were plotted against the blockage ratio no significant trend in the data could be observed.

C. Free convection effect

The boundary effect in mixed laminar convection around a horizontal cylinder can be estimated using the parameter $|Gr|/Re^2$. Using the lowest free stream velocity $U_\infty=1.02$ cm/s and the maximum $\Delta T=2.7°C$ in this study, the value for $|(Gr)_{Ds}|/Re^2_{Ds}$ is found to be 0.64 and the effect of free convection in heat transfer result is estimated to be less than one percent. It is noted that the free convection effect becomes significant when the parametric value is greater than 1.92.

D. The effect of longitudinal vortices

In the range of Reynolds number Re_{Ds} considered in this study, one may expect the appearance of the longitudinal vortices near the forward stangation point[42]. However, visual observation shows that no traces of longitudinal vortices on the ice surface can be detected.

E. The effect of free stream turbulence

The effect of free stream turbulence on heat transfer results for the present problem has been studied by Kestin and Wood[43], Smith and Kuethe[44], Drun, Diepand Kestin[45], Seban[46], Appelqvist[47], Kayala[48] and others. The results from this study and previous results are plotted in Fig. 6 in the form of modified Frössling number $Fr^*=(Nu)_{Ds}/Re^{1/2}_{Ds}/(Pr)^{0.4}$ versus the parameter involving turbulent intensity $Tu\,(Re)^{1/2}_{Ds}$ for comparison. The modified Frössling number is used in order that the empirical correlation of Kestin and Wood[43] and the semi-empirical correlation of Smith and Kuethe[44] may predict the general qualitative trend of

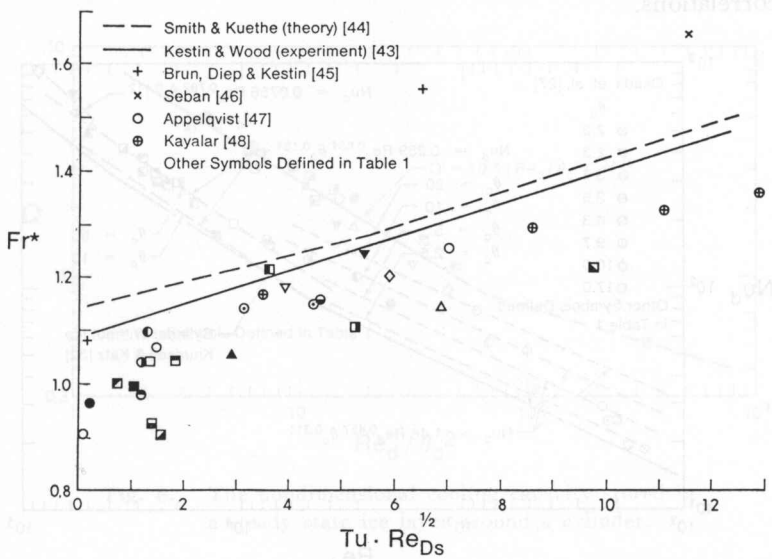

Fig. 6. The effect of free steam turbulence on heat transfer at the forward stagnation point.

the present data and also so that the present data is consistent with previous data when turbulence is accounted for. There is still a considerable scatter in the data which may in part be attributed to the effects of the differing length scales of the turbulence as has been suggested by Kestin et al,[49] Smith and Kuethe[44], Zapp[50] and Sunden[51].

4.3 Average heat transfer

The average Nusselt number Nu_d as a function of a the Reynolds number is shown in Fig. 7 where the results from Okada et al.[27] for a low Reynolds number range are also plotted for reference. The experimental correlation equations for the average Nusselt number Nu_d using the parameters Re_d and θ_c are obtained by using the least square method. The results are:

$$Nu_d = 1.46 Re_d^{0.457} \theta_c^{0.311}, \quad 2 < \theta_c < 20, \quad Re_d < 5 \times 10^3 \tag{7}$$

$$Nu_d = 0.289 Re_d^{0.637} \theta_c^{0.151}, \quad 6 < \theta_c < 76, \quad 5 \times 10^3 < Re_d < 5 \times 10^4 \tag{8}$$

$$Nu_d = 0.0756 Re_d^{0.792} \theta_c^{0.112}, \quad 40 < \theta_c < 65, \quad Re_d > 5 \times 10^4 \tag{9}$$

In the low Reynolds number range $Re_d < 5 \times 10^3$ the standard deviation of the experimental data from equation (7) is ± 11 percent. In the range $5 \times 10^3 < Re_d < 5 \times 10^4$ where the influence of the turbulent boundary layer appears, the experimental data deviation from rquation (8) is 7 percent. For $Re_d > 5 \times 10^4$.there is a lack of sufficient experimental data, but the data agree with equation (9) within ± 5 percent.

Also shown on Fig. 7 is the standard correlation used for cylinders without ice[53]. It can be seen that this value is reached for $\theta_c = 2$ in equation (7) and $\theta_c = 10$ in equation (8). These values of θ_c represent the lower limit of applicability of these correlations.

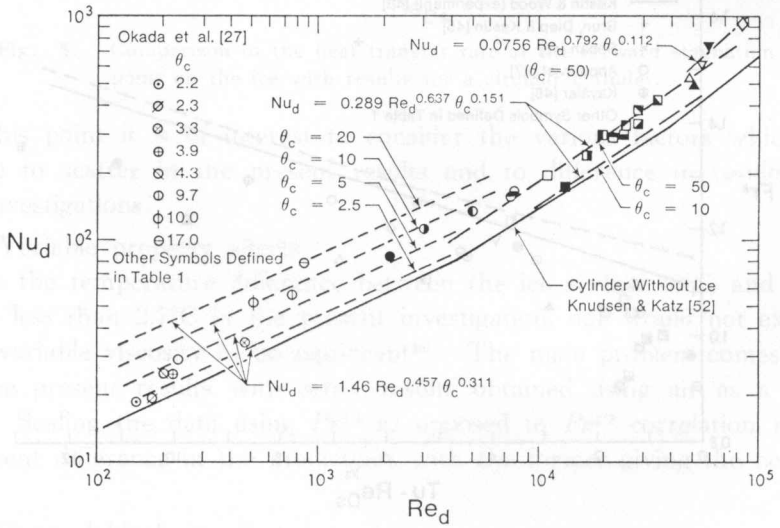

Fig. 7. The influence of the ice layer on the average heat transfer rate to the cylinder.

4.4 The amount of ice growth around the cylinder

In applications where cooling capacity is stored by growing ice, for example in some types of water chillers, an important factor to be known is the total amount of cooling capacity stored in the ice. The storage, Q, per unit length of pipe is then

$$Q=\gamma_s L A_s \tag{10}$$

where A_s is the cross sectional area of ice. In this equation the sensible heat storage has been neglected as it is usually small compared to the latent heat of fusion. Equation (10) can be rewritten in a dimensionless form as

$$Q'=\frac{4Q}{\pi d^2\gamma_s L}=\frac{4A_s}{\pi d^2} \tag{11}$$

In Figure 8, Q' has been plotted as a function of the parameter Re_d/θ_c^2. This parameter would be expected to be a precisely valid correlation parameter only if the flow was entirely laminar[19], however, it appears to be reasonably effective in this case as well. The correlation equation is given by

$$Q'=10.6(Re_d/\theta_c)^{-0.612} \tag{12}$$

In the range $3<Re_d/\theta_c^2<50$ the standard deviation between the experimental data and equation (12) is ± 11 percent.

For values of Re_d/θ_c^2 much greater than 50 the ice layer becomes too thin for accurate measurement; however, the one data point that was taken at a value of 300 suggests that the correlation will underpredict that extent of ice growth for very thin layers. At the other limit that is $Re_d/\theta_c^2\to 0$ ($Re_d\to 0$ or $\theta_c\to\infty$) one must consider free convection effects.

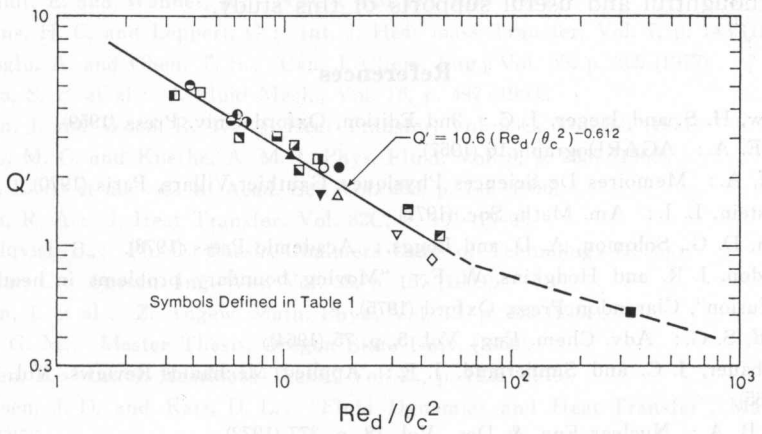

Fig. 8. The nondimensional cooling capacity stored in a steady state ice layer around a cylinder.

5. Conclusion

It was found that local and average heat transfer rates at the ice-water interface of an ice layer grown in a cricular cylinder could be determined directly from a photograph showing the shape of the ice layer. The calculation involved first solving for the temperature field in the ice using a point matching method and then extracting the temperature gradients and heat transfer rates at the ice-water interface. The method was simple and convenient to use and thus may find application for other geometries where ice growth is studied.

Using the technique results were obtained for the variation in local heat transfer over the ice surface in various Reynolds number regimes between $Re_d = 2.3 \times 10^2$ to 8.6×10^4. The local heat transfer results can be used to imply points of flow separation and transition on the ice. From the present results it would appear that a laminar to turbulent boundary layer transition occurs on the ice layer around a cylinder at Reynolds numbers as much as an order of magnitude lower than it would for a circular cylinder without ice. This observation is consistent with previous observations of transition on an ice layer grown on a flat plate and appears to be due to the interaction of the flow and the shape of the ice layer.

Correlations were obtained for the average heat transfer coefficient to a cylinder with ice growth and for the total quantity of cooling capacity that could be stored in the ice.

Acknowledgement

The author wishes to express his sincere thanks to Prof. K. C. Cheng and Prof. R. R. Gilpin, Dept of Mechanical Engineering, The University of Alberta, for their thoughtful and useful supports of this study.

References

1) Carslaw, H. S. and Jaeger, J. C.: 2nd Edition, Oxford Univ. Press (1959).
2) Brun, E. A.: AGARDograph 16 (1957).
3) Datzeff, A.: Memoires De Sciences Physiques, Gauthier-Villars, Paris (1970).
4) Rubinstein, L. I.: Am. Math. Soc. (1971).
5) Wilson, D. G., Solomon, A. D. and Boggs.: Academic Press (1978).
6) Ockendon, J. R. and Hodgkins, W. F.: "Moving boundary problems in heat flow and diffusion", Clarendon Press, Oxford (1975).
7) Bankoff, S. G.: Adv. Chem. Eng., Vol. 5, p. 75 (1964).
8) Muehlbauer, J. C. and Sunderland, J. E.: Applied Mechanics Reviews, Vol. 18, p. 951 (1965).
9) Boley, B. A.: Nuclear Eng. & Des., Vol. 18, p. 377 (1972).
10) Lock, G. S. H.: Trans. N.E. Coast Inst. Engrs. Shipbuilders, Vol. 88, p. 175 (1972).
11) Lock, G. S. H.: Int. Heat Transfer Conf. Vol. 6, p. 12 (1974).
12) Minsk.: CRREL Report, p. 77 (1977).
13) Ashton, G. D. and Kednedy, J. F.: J. Hydaul, Div. ASCE, Vol. 98, p. 1603 (1972).
14) Hirata, T., Gilpin, R. R. and Cheng, K. C.: Int. J. Heat Mass Trans., Vol. 22, P. 1435

(1979).
15) Gilipin: AIChE Symposium Series, Vol. 75. p. 89 (1979).
16) Gilipin, R. R., Hirata, T. and Cheng, K. C.: J. Fluid Mech., Vol. 99, p. 619 (1980).
17) Zerkle, D. and Sunderland, J. E.: J. Heat Transfer, Vol. 90, p. 183 (1968).
18) Mulligan, J. C. and Jones, D. D.: Int. J. Heat Mass Transfer, Vol. 19, p. 312 (1976).
19) Hirata, T. Gilpin, R. R. and Cheng, K. C.: Int. J. Hest Mass Trans., Vol. 22, p. 1425 (1979).
20) Savino, J. M. and Siegel, F.: NASA TND-4015 (1967).
21) Kishinami, K. and Saito, T.: Reports of Faculty of Engineering, Hokkaido Univ., No. 63, p. 1 (1971).
22) Kishinami, K.: Refrigeration, Vol. 51, p. 259 (1976).
23) Saitoh, T.: Appl. Sci. Res., Vol. 32, P. 429 (1976).
24) Ramsey, J. W., Sparrow, E. M. and Varejas, L. M. C.: J. Heat Transfer, Vol. 101. p. 732 (1979).
25) Bathelt, A. G. Viskanta, R. and Leidenfrost, W.: J. Fluid Mech., Vol. 90 (1979).
26) Carlson, F. N. Ph. D.: Thesis, University of Connecticut (1975).
27) Okada, M. et al.: Bulletin of the JSME, Vol. 21, p. 1514 (1978).
28) London, A. L. and Seban, R. A.: Trans. ASME, Vol. 65, p. 771 (1943).
29) Tien, L. C. and Churchill, S. W.: AIChE Journal, Vol. 11, P. 790 (1965).
30) Shin, Y. P. and Tsay, S. Y.: Chem. Eng. Sci., Vol. 26, p. 809 (1971).
31) Gupta, J. P.: Chem. Eng. Sci., Vol. 28, p. 1627 (1973).
32) Morgun, V. T.: Adv. Heat Transfer, Vol. 11, p. 199 (1975).
33) Giedt, W. H.: Trans. ASME, Vol. 71, p. 375 (1949).
34) Giedt, W. H.: J. Aeronaut. Sci., Vol. 18, p. 725 (1951).
35) Eckert, E. R. G. and Soehngen, E.: Trans. ASME, Vol. 74, p. 343 (1952).
36) Cheng, K. C. and Hwang, G. J.: AIChE Journal, Vol. 14, p. 510 (1968).
37) Hilderbrand, F. B.: "Advanced Calculus for Applications", Prentice-Hall (1962).
38) Squire, H. B.: "Modern Development in Fluid Dynamics", Vol. 2, Oxford Univ. Press, p. 632 (1938).
39) Schmidt, E. and Wanner, K.: NACA TM No. 1050 (1943).
40) Perkins, H. C. and Leppert, G.: Int. J. Heat mass Transfer, Vol. 7, p. 143 (1964).
41) Mucoglu, A. and Chen, T. S.: Can. J. Chem. Eng., Vol. 55, p. 265 (1977).
42) Sutera, S. P. et al.: J. Fluid Mech., Vol. 16, p. 497 (1963).
43) Kestin, J. and Wood, R. T.: J. Heat Transfer, Vol. 93C, Vol. 321 (1971).
44) Smith, M. C. and Kuethe, A. M. : Phys. Fluid, Vol. 9, p. 2337 (1966).
45) Brun, E. A. et al.: C. R. Acad. Sci. Vol. 263, p. 742 (1966).
46) Seban, R. A.: J. Heat Transfer, Vol. 82C, P. 101 (19-0).
47) Appelqvist, B.,: Ph. D. Thesis, Chalmers Univ. of Technology (1965).
48) Kayalar, L.: Forsch. Ing.-Wes. Vol. 35, p. 157 (1969).
49) Kestin, J. et al.: Z. Angew. Math. Phys., Vol. 12, p. 115 (1961).
50) Zapp, G. M.: Master Thesis, Oregon State Univ. (1950).
51) Sunden, B.: Int. J. HeatMass Trans., Vol. 22, p. 1125 (1979).
52) Knudsen, J. D. and Katz, D. L.: "Fluid Dynamics and Heat Transfer", MacGraw-Hill (1985).